How to cite: Angew. Chem. Int. Ed. 2023, e202306155
doi.org/10.1002/anie.202306155

MOF Films

Metal-Organic Framework Thin Films as Ideal Matrices for Azide Photolysis in Vacuum

Jimin Song, Xiaojuan Yu, Alexei Nefedov, Peter G. Weidler, Sylvian Grosjean, Stefan Bräse, Yuemin Wang, and Christof Wöll**

Abstract: Studies on reactions in solutions are often hampered by solvent effects. In addition, detailed investigation on kinetics is limited to the small temperature regime where the solvent is liquid. Here, we report the in situ spectroscopic observation of UV-induced photochemical reactions of aryl azides within a crystalline matrix in vacuum. The matrices are formed by attaching the reactive moieties to ditopic linkers, which are then assembled to yield metal–organic frameworks (MOFs) and surface-mounted MOFs (SURMOFs). These porous, crystalline frameworks are then used as model systems to study azide-related chemical processes under ultrahigh vacuum (UHV) conditions, where solvent effects can be safely excluded and in a large temperature regime. Infrared reflection absorption spectroscopy (IRRAS) allowed us to monitor the photoreaction of azide in SURMOFs precisely. The in situ IRRAS data, in conjunction with XRD, MS, and XPS, reveal that illumination with UV light first leads to forming a nitrene intermediate. In the second step, an intramolecular rearrangement occurs, yielding an indoloindole derivative. These findings unveil a novel pathway for precisely studying azide-related chemical transformations. Reference experiments carried out for solvent-loaded SURMOFs reveal a huge diversity of other reaction schemes, thus highlighting the need for model systems studied under UHV conditions.

Introduction

The exceptional chemical and physical properties of metal–organic frameworks (MOFs) account for their significant potential as functional materials for various innovative applications.[1] These crystalline, porous coordination polymers are assembled with extremely high surface area, ordered porosity, and customizable organic functions. In the field of catalysis, the presence of isolated metal cation nodes in MOFs renders them highly promising as single-site catalysts.[2] Furthermore, MOF materials offer a versatile scaffold for embedding diverse functional groups, which can be precisely anchored at well-defined linker positions and homogeneously dispersed within the framework. This inherent tunability of MOFs provides a robust platform for driving a wide range of reactions, including photocatalytic CO_2 reduction[3] and multicomponent organic photoreactions.[4]

The chemistry of azide groups has garnered growing attention in recent years due to their versatile applications as "high-energy" functional groups.[5] Organic azides are well-recognized as potent precursors that can be transformed through thermal[6] and/or photo-decomposition or addition reactions into a wide range of valuable molecules, including amines, isocyanates, and other heterocyclic compounds containing nitrogen.[5] In addition, the photolysis of aryl azides has also found compelling applications for photoresists,[7] in which aryl azides are efficiently utilized in photoaffinity labeling. While the photolysis of matrix-isolated organic azides has been reported,[8] most studies on the photochemistry of azides have primarily focused on solvent-based systems. Given their significance in click chemistry, diverse organic azides have been integrated into MOFs, presenting an intriguing avenue for exploration.[9] However, there is still a lack of fundamental insights into the microscopic mechanisms of azide photoreactions. Compared to the traditional approach to studying reactions in solvents or in inert cryogenic matrices,[5,10] the highly ordered, crystalline, and porous nature of MOFs offers great potential for an in-depth investigation of organic reaction mechanisms. In particular, the open structure of the frameworks allows to add further reactants in a straightforward

[*] J. Song, Dr. X. Yu, Dr. A. Nefedov, Dr. P. G. Weidler, Dr. Y. Wang, Prof. Dr. C. Wöll
Institute of Functional Interfaces (IFG), Karlsruhe Institute of Technology (KIT)
Hermann-von-Helmholtz-Platz1, 76344 Eggenstein-Leopoldshafen (Germany)
E-mail: yuemin.wang@kit.edu
christof.woell@kit.edu

Dr. S. Grosjean, Prof. Dr. S. Bräse
Institute for Biological and Chemical Systems (IBCS-FMS) and IBG3-SML, Karlsruhe Institute of Technology (KIT)
Hermann-von-Helmholtz-Platz1, 76344 Eggenstein-Leopoldshafen (Germany)

Prof. Dr. S. Bräse
Institute for Organic Chemistry (IOC), Karlsruhe Institute of Technology (KIT)
Fritz-Haber-Weg 6, 76131 Karlsruhe (Germany)

fashion, an option which is difficult to realize in conventional cryogenic matrix isolation spectroscopy.

In comparison to powders, the most common form of these crystalline coordination networks, surface-mounted MOF thin films (SURMOFs), grown on solid substrates via the liquid-phase quasi-epitaxy approach,[11] exhibit low defect densities[2d] and well-defined morphology. In addition, surface barriers often limiting the uptake of guest molecules can be studied and either eliminated or strongly reduced.[12] As a result, SURMOFs represent an excellent model system that is well-suited for surface characterizations and fundamental investigations.[13]

Herein, we report the synthesis of an azide-containing Cu-(Da-SBDC) SURMOF. We have established a solvent-free model system using the azide-SURMOF to study photochemical reactions of azide employing a multi-technique approach including ultrahigh vacuum infrared reflection absorption spectroscopy (UHV-IRRAS), X-ray diffraction (XRD), mass spectrometry (MS), and X-ray photoelectron spectroscopy (XPS). The comprehensive results obtained from this study provide detailed insights into the photoactivation of azide and the reaction mechanism in SURMOFs (Figure 1) while eliminating unwanted effects of the solvent.

Results and Discussion

Highly oriented and crystalline Cu-(Da-SBDC) SURMOFs were grown on -COOH functionalized gold surfaces via a layer-by-layer deposition (CCDC-2264560).[14] The corresponding XRD results confirmed that the obtained structure of the SURMOFs was highly crystalline, with the (001) crystallographic direction oriented normal to the substrate (Figure S1).[14] Scanning electron microscope (SEM) images revealed the thin film's flat and smooth surface morphology (Figure S2). The IRRAS data exhibited the characteristic vibrational band at 2127 cm^{-1} corresponding to the azide group stretching mode $\nu(N_3)$ (Figure S4). Additional IR bands at 1602 and 1428 cm^{-1} are ascribed to the carboxylate-related vibrations ν_{as}(OCO) and ν_s(OCO), respectively. The 1558 cm^{-1} band is indicative of the stretching vibration

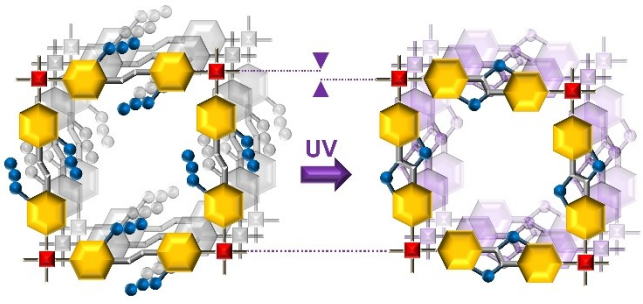

Figure 1. Schematic illustration of intramolecular photoreactions of azide in metal–organic frameworks. Red square: Cu paddle wheels; Yellow hexagon: benzene ring; Blue dot: nitrogen atom; Gray bar: carbon bond.

ν(C–C) from the phenyl ring. These vibrational bands confirmed the structure of the Da-SBDC linker, as depicted in Figure 2d. With Cu–Cu paddle wheels as the metal node and Da-SBDC as the linker, the Cu–(Da–SBDC) MOF structure exhibits the same topology as SURMOF-2.[15]

The photochemistry of azides was characterized in situ using a proprietary multipurpose UHV apparatus dedicated to IRRAS measurements with monolayer sensitivity.[16] Figure 2 shows the time-resolved UHV-IRRAS data obtained under UV irradiation of Cu-(Da-SBDC) SURMOF. Upon illumination with UV light at 298 K, the azide $\nu(N_3)$ band at 2127 cm^{-1} gradually decreased in intensity (Figure 2a). Similarly, the band at 3058 cm^{-1}, assigned to the stretching vibration of C–H groups in –HC=CH– (see Figure 2d), also showed a gradual attenuation in intensity. Notably, the benzene ring ν(C–H) vibrations at 2925 and 2855 cm^{-1}, as well as the ν(C–C) vibration at 1558 cm^{-1}, remained unchanged in intensity (Figures 2a, S5). Importantly, the UV illumination led to the appearance of one new vibrational band at 1250 cm^{-1} (Figure S5). As discussed below, we assign this peak to the stretching mode ν(C–N) in the pyrrole-containing indoloindole rings formed during the photochemical reaction. This assignment follows the previous observation.[17]

Based on a quantitative analysis, the time dependence of the $\nu(N_3)$ band intensity at different temperatures, as shown in Figure 2b, reveals a continuous decrease under UV irradiation at 298 K, with the band almost completely disappearing after 20 min. At lower temperatures, the decrease is slighter. The reaction rates, shown in Figure 2c, exhibit an initial increase followed by a steep decrease, with the highest reaction rates observed at 298 K. In Figure 2d–f, the different vibrational bands are shown in more detail. The decreasing intensity for the ν(C–H) band at 3058 cm^{-1} in –HC=CH– showed a similar trend to the $\nu(N_3)$ band at 2127 cm^{-1}. The consumption rate of both bands increases initially for the first 2.5 minutes, reaching their maximum, then decreases after that. This finding indicated an addition reaction between the two groups in MOF, –HC=CH– (3058 cm^{-1}) and activated azide (2127 cm^{-1}). Importantly, the attenuation of both bands is accompanied by a gradual increase in the intensity of the ν(C–N) mode at 1250 cm^{-1} in the indoloindole group (Figure S5), providing further evidence for the subsequent reaction with the adjacent –HC=CH– groups after photoactivation of the azide groups.

The dipole character of azides makes them capable of undergoing cycloaddition reactions with alkenes. However, the possibility of the formation of dihydroazepine with the insertion of the N atom into the aryl ring can be ruled out in the present work, as dihydroazepine motifs would exhibit very strong vibrational peaks around 1890 cm^{-1} if they were present.[18] In our case, however, no obvious peaks were present at 1890 cm^{-1}, nor was the change in the 1558 cm^{-1} band from the phenyl ring's (ν(C–C) vibration. This indicates that a rearrangement of aryl nitrenes[19] did not occur in this system. Additionally, in the presence of water, alkenyl aryl azide could provide access to substituted azepinones by ring expansion. While under UHV conditions

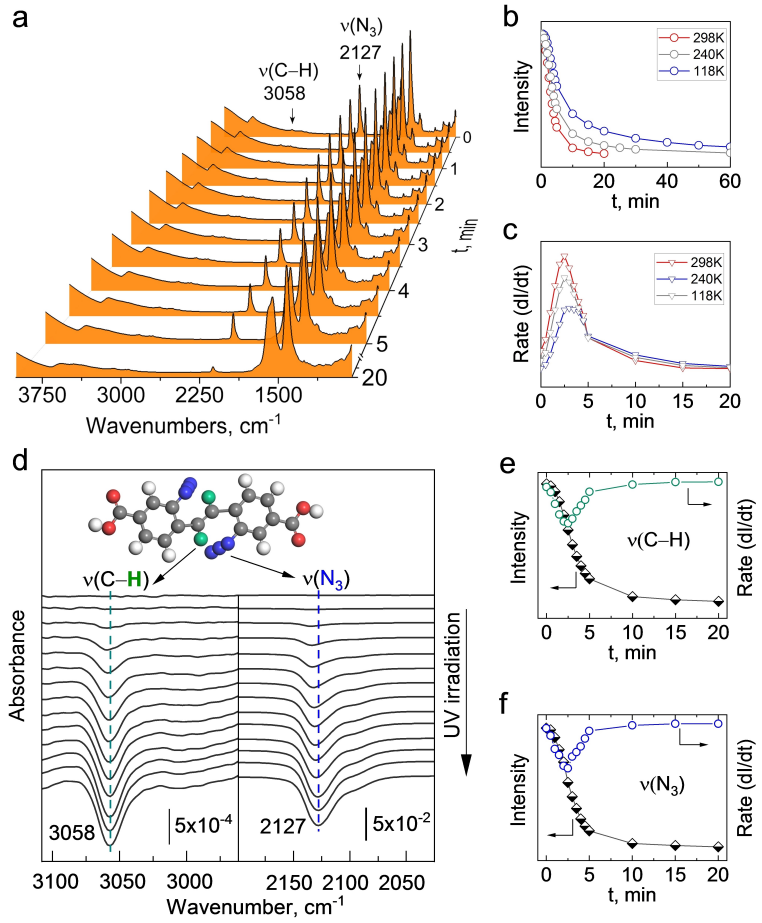

Figure 2. In situ UHV-IRRAS results of photoreactions. **a)** Time-resolved full range IRRAS data under UV illumination (254 nm) at 298 K. **b)** Intensity evolution of the 2127 cm^{-1} band at different temperatures (298, 240 and 118 K) as function of UV irradiation time. **c)** Consumption rate of the 2127 cm^{-1} band at different temperatures (298, 240 and 118 K) as function of UV irradiation time. **d)** UV-induced spectral evolution of the ν(C–H) and ν(N_3) vibrations in IRRA difference spectra at 298 K. **e)** UV-induced intensity and rate (d*I*/dt) evolution of the ν(C–H) vibration at 298 K. **f)** UV-induced intensity and rate (d*I*/dt) evolution of the ν(N_3) vibration at 298 K.

at $\sim 1 \times 10^{-10}$ mbar, water's influence could also be eliminated.

The loss of nitrogen from organic azides results in uncharged monovalent nitrene intermediates, which have a short lifetime (only several microseconds) with activation energies for nitrogen elimination on the order of −40 kcal/mol.[20] Under UV irradiation, azide group photolysis may result in N atom insertion into the phenyl ring motif, generating an azepine.[19] The solution-phase photochemistry of phenyl azide is reported to be temperature dependent.[21] For example, the photolysis of phenyl azide in the presence of diethylamine at ambient temperature yields azepine, but lowering the temperature suppresses the yield of azepine, and at temperatures below 160 K, azobenzene, the product of triplet nitrene dimerization, is produced.

In this study, photoreaction experiments were conducted at different temperatures (298, 240, and 118 K) on the solvent-free azide-SURMOFs, and it was found that UV irradiation at lower temperatures leads to slower transformation but still follows the same trend of evolution as shown in Figure 2b, c, and Figure S6. In addition, comparing the IRRAS spectra acquired in the ambient atmosphere (Figure S7), no obvious differences were observed except that there was much more noise in the latter. This also indicates that O_2 and moisture are not involved in the reaction pathway. These findings reveal that the solvent-free photochemical reactions of azides in MOFs differ from those in solutions. In the well-designed azide-SURMOFs used in this study, organic linkers serve as isolated functional groups for intramolecular reactions, while intermolecular side reactions such as the formation of azo benzenes are avoided.

The photochemical reactions of azides in SURMOFs were further characterized by recording X-ray photoelectron spectra before and after UV illumination. Figure 3a shows a doublet in the N 1s region at 403.6 and 400.2 eV, attributed to the central electron-deficient nitrogen species and two lateral nitrogen atoms, respectively.[22] The relative peak area ratio of the two N components is close to 1:2, as expected. In the deconvoluted spectrum, a weak signal was resolved at 398.9 eV, which is ascribed to a small fraction of decomposed azide. After UV illumination, the bands at 403.6 and 400.2 eV could no longer be detected (Figure 3a), indicating a complete transformation of azide groups. A quantitative analysis yields a loss of about 60 % of the

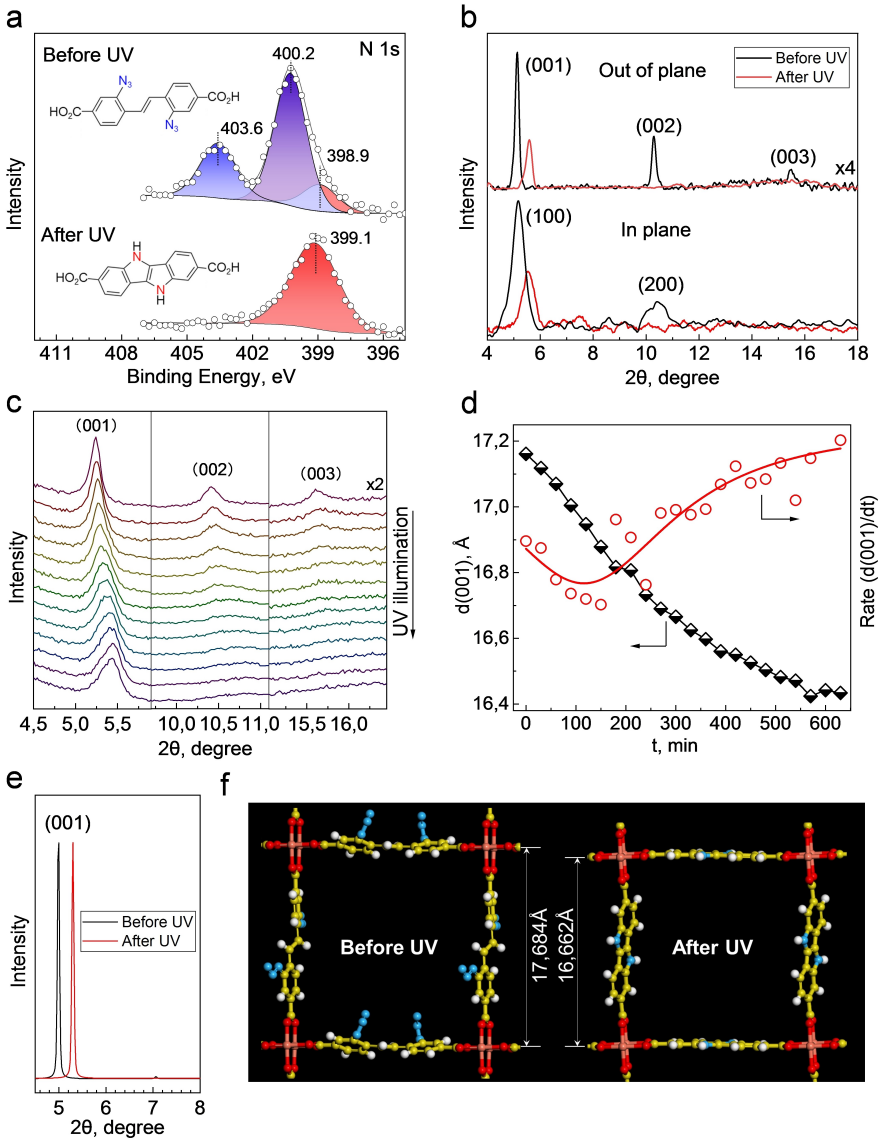

Figure 3. Chemical and structural properties of azide-SURMOF characterized by XPS and in situ XRD. **a)** XPS N 1s spectra before and after UV illumination (298 K, 60 min). **b)** Out-of-plane and in-plane XRD patterns recorded before and after UV illumination (298 K, 60 min). **c)** In situ XRD of Cu(Da-SBDC) SURMOF under UV illumination at 298 K. **d)** Evolution of the d-spacing of the (001) plane (d(001)) and the rate (d(001)/dt) as function of UV irradiation time. **e)** Simulated XRD patterns before and after UV illumination. **f)** Simulated structural changes of azide-SURMOFs before and after UV illumination.

nitrogen atoms, in agreement with the UV-induced decomposition of the azide ($-N_3$) into gaseous N_2 and a remaining N species.

One of the unique advantages of SURMOFs is their high crystallinity, which allows for detailed characterization of structural changes. The XRD results recorded before and after UV illumination (Figure 3b) provided information on the length changes of the azide-containing organic linkers. The out-of-plane and in-plane XRD patterns revealed the presence of well-defined diffraction peaks, indicating that the crystallinity of azide-SURMOFs was largely preserved during the photochemical reaction. Importantly, the XRD peak positions shifted to higher angles for the (001) peak from 5.1 to 5.8 degrees (Figure 3b). This shift directly implies a shortening of the organic linkers upon UV illumination. The second and third-order peaks (002) and (003) almost disappeared, which can be explained by the gradual tilting away of the surface normal direction of the (001) plane from the direction of the scattering vector H_{001} based on the Laue equation. More ring strain would be imposed on the structure when cycloaddition reactions happened in MOFs under UV light.[23] As discussed above, the IR spectral evolution observed for azide groups as well as C=C and C–N vibrations (Figure 2) reveals the addition reaction between the azide and the C=C groups and the compressing effect of the strain imposed by the lattice distortion. The corresponding SEM images (Figure S3) showed no obvious variation, supporting structural stability.

In situ XRD experiments were performed to investigate the time-resolved evolution of the azide-SURMOF structure (Figure 3c). We note that weaker UV light intensity was required to slow down the photo reaction, thus enabling the viable collection of XRD patterns. The intensity of (001) plane decreased in the first 200 min. Then it maintained almost unchanged when the azide groups were exhausted, consistent with the ambient IRRAS data in Figure S7. As shown in Figure S8, 60 % of the intensity remained in the next 400 min, indicating the structural changes and proper stability during the photochemical reaction. The (001) diffraction peak shifted gradually from 5.2 to 5.5 degrees in a 600 min in situ observation, with the calculated lattice spacing decreased from 17.161 to 16.434 Å (Figure 3d). We suggest that the distortion of the lattice due to the shrinking of MOF linkers leads to a significant reaction rate increase for azide. This is further supported by the time evolution of the (001) peak shifting rate under UV illumination and the change of the stress/strain parameter Δd/d (Figure S9). We note that the ring strain was proved to accelerate azide-alkyne cycloaddition.[24] Upon forming a cyclization structure between one of the two azide groups in the Da-SBDC linker and the adjacent C=C double bond, the other azide group could be promoted to react with another neighboring C=C group. This finding is also consistent with those observed in IRRAS, in which the consuming rates of the ν(N3) band at 2127 cm^{-1} and the ν(C–H) band in –HC=CH– at 3058 cm^{-1} followed the same trend (Figure 2e, f).

The simulated XRD patterns (Figure 3e) for these structures agreed well with the experimental findings for both samples before and after UV illumination (CCDC-2264561).[14] The simulated lattice spacing decreased from 17.684 to 16.662 Å (Figure 3f), in line with the observed structural changes during the photochemical reaction.

Based on these observations, it is proposed that an indole component was formed in the SURMOF along with the UV illumination. Indole motifs are important moieties in the pharmaceutical industry. They can be synthesized through various metal-catalyzed and photochemical methods, such as irradiation of vinyl and aryl azides with visible light in the presence of Ru photocatalysts or from dienyl azides at room temperature catalysed by ZnI_2 or $Rh_2(O_2CC_3F_7)_4$.[25] In addition, the thermal conversion of stilbene bisazides to indoloindoles has also been reported.[26] Notably, these experiments were performed in the organic solvents. In our case, UV light is the only intriguing factor in boosting indole formation without catalysts and solvents.

Formal insertion into C(sp2)–H bonds is a frequently used reaction that partly follows the cycloaddition principle. Thus indoles, carbazoles and other heterocycles can be formed. Again, here in our systems, the photochemical reactions of azide occur in activated SURMOFs, in which the solvent effects and any side reactions are avoided. To illustrate this important point, the impact of diverse solvents on the photolysis of azides in SURMOFs has been investigated (see Figure S10). After the reactions for each solvent, in some cases new features were observed in the IR data (Figure 4). However, the effect of the solvent is not limited to yielding different products originating from the

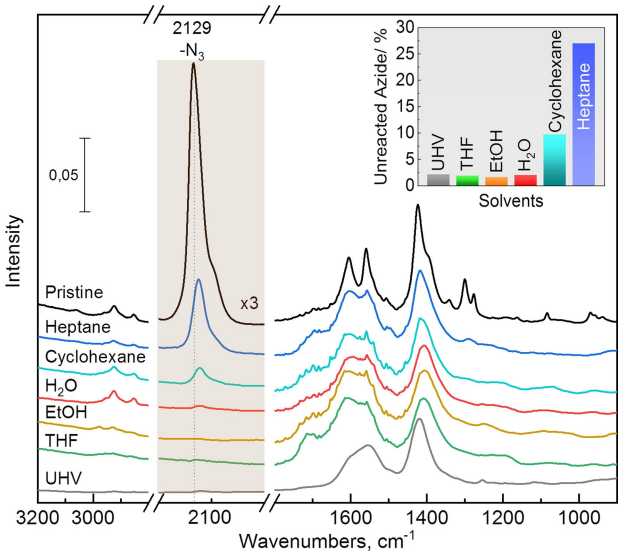

Figure 4. Comparison of azide photolysis in UHV and solvents. IRRAS data of azide-SURMOFs after UV illumination (254 nm) at 298 K for 50 min in UHV and various solvents including H_2O, tetrahydrofuran (THF), ethanol (EtOH), cyclohexane, and heptane. The inset shows the concentration of remaining azide based on a quantitative analysis of the azide ν(N_3) band intensity at 2129 cm^{-1}.

reaction of the intermediate nitrene with different molecules, but also the initial photolysis of azide to form nitrene is affected. This is evidenced by the inset in Figure 4, which shows that the intensity decrease of the azide band at 2129 cm^{-1} is much slower in heptane and cyclohexane than in UHV (and the other solvents). The origin of this decrease might be intermolecular interactions (including the formation of hydrogen bonds) between the solvent and the nonpolar azide moiety. In addition, in case of water and ethanol a hydrogen transfer might occur as reported previously for similar systems.[27] Certainly, for the solvents the products are different from that obtained under UHV conditions, e.g. inter- and intramolecular CH activation or ring expansion to yield azepinones might take place.

Overall, the comprehensive results provided insights into the photoreaction mechanism of azide in the Cu(Da-SBDC) SURMOF. In the first step, the photoreaction of azide occurs immediately upon UV illumination, forming nitrene species. In the second step, the nitrene species reacts with adjacent C=C groups in the MOF, forming an indole component through intramolecular amination. To further verify this conclusion, mass spectrometry (MS) data were obtained to study the transformation of organic linkers. As illustrated in Figure S11, compounds with a molecular weight of 349 dominated before UV illumination, while compounds with a molecular weight of 293 increased significantly after UV illumination. This indicates the structural change of MOF linkers and the formation of a pyrrole-containing indolo[3,2-b] indole[28] in the photoreaction process.

Conclusion

In summary, we have provided direct evidence for the structural and chemical changes during photoreactions of azide in crystal-stable Cu(Da-SBDC) SURMOFs by applying UHV-IRRAS. The crystalline structure acts as a scaffold where photochemical reactions occur, and the functionalized organic linkers are targeted as probe molecules to investigate the reaction mechanism. After forming radical nitrene under UV irradiation, an addition reaction occurs between the nitrene and adjacent C=C double bonds instead of ring expansion between the nitrene and phenyl ring. During this reaction, O_2 and moisture are not involved whenever testing in an atmosphere or UHV. The proposed mechanism involving the reaction between an azide and C=C double bonds is further supported by in situ XRD, XPS, and MS. As a result of the interplay between addition reaction and lattice strains, the photoreaction proceeds gradually faster and then slowing down. This work provides a novel strategy to characterize SURMOFs and to understand in-depth organic reaction mechanisms without any solvent effect. It is possible to use the structure–reactivity data to qualitatively predict the behavior of the compounds produced upon photolysis of azide. Additionally, a UV-activated route offers an alternative post-synthetic modification because the target function is added after the MOF lattice is formed without altering the topology of the parent material. Here it also showed that the pore control of MOF is viable via a simple illumination treatment, which opens the gate to the successful MOF application in controllable sensors, adsorption, and separation.

Acknowledgements

We acknowledge financial support by the Deutsche Forschungsgemeinschaft (DFG, German Research Foundation) under Germany's Excellence Strategy via the Excellence Cluster "3D Matter Made to Order" (3DMM2O, EXC-2082/1-390761711, Thrust A1 and A3) and the SFB 1441 (Project-ID 426888090). J.S. is grateful for Ph.D. fellowships from the China Scholarship Council (CSC). Open Access funding enabled and organized by Projekt DEAL.

Conflict of Interest

The authors declare no conflict of interest.

Data Availability Statement

The data that support the findings of this study are available in the supplementary material of this article.

Keywords: Azide Photolysis · IRRAS · Metal Organic Frameworks · Photoreaction · Reaction Mechanisms

[1] a) H. Furukawa, K. E. Cordova, M. O'Keeffe, O. M. Yaghi, *Science* **2013**, *341*, 1230444; b) H. C. Zhou, J. R. Long, O. M. Yaghi, *Chem. Rev.* **2012**, *112*, 673–674; c) Y. Cui, B. Li, H. He, W. Zhou, B. Chen, G. Qian, *Acc. Chem. Res.* **2016**, *49*, 483–493.

[2] a) J. M. Thomas, R. Raja, D. W. Lewis, *Angew. Chem. Int. Ed.* **2005**, *44*, 6456–6482; b) S. M. Rogge, A. Bavykina, J. Hajek, H. Garcia, A. I. Olivos-Suarez, A. Sepúlveda-Escribano, A. Vimont, G. Clet, P. Bazin, F. Kapteijn, *Chem. Soc. Rev.* **2017**, *46*, 3134–3184; c) Y. Wang, C. Wöll, *Catal. Lett.* **2018**, *148*, 2201–2222; d) W. Wang, D. I. Sharapa, A. Chandresh, A. Nefedov, S. Heißler, L. Heinke, F. Studt, Y. Wang, C. Wöll, *Angew. Chem. Int. Ed.* **2020**, *59*, 10514–10518.

[3] G. Lan, Z. Li, S. S. Veroneau, Y.-Y. Zhu, Z. Xu, C. Wang, W. Lin, *J. Am. Chem. Soc.* **2018**, *140*, 12369–12373.

[4] a) Y.-Y. Zhu, G. Lan, Y. Fan, S. S. Veroneau, Y. Song, D. Micheroni, W. Lin, *Angew. Chem. Int. Ed.* **2018**, *57*, 14090–14094; b) H. Yonezawa, S. Tashiro, T. Shiraogawa, M. Ehara, R. Shimada, T. Ozawa, M. Shionoya, *J. Am. Chem. Soc.* **2018**, *140*, 16610–16614; c) S. Diring, D. O. Wang, C. Kim, M. Kondo, Y. Chen, S. Kitagawa, K.-i. Kamei, S. Furukawa, *Nat. Commun.* **2013**, *4*, 2684; d) K. K. Tanabe, C. A. Allen, S. M. Cohen, *Angew. Chem. Int. Ed.* **2010**, *49*, 9730–9733; e) S. Kusaka, R. Matsuda, S. Kitagawa, *Chem. Commun.* **2018**, *54*, 4782–4785; f) T. Luo, L. Li, Y. Chen, J. An, C. Liu, Z. Yan, J. H. Carter, X. Han, A. M. Sheveleva, F. Tuna, E. J. L. McInnes, C. C. Tang, M. Schröder, S. Yang, *Nat. Commun.* **2021**, *12*, 3583.

[5] S. Bräse, C. Gil, K. Knepper, V. Zimmermann, *Angew. Chem. Int. Ed.* **2005**, *44*, 5188–5240.

[6] M. Schock, S. Bräse, *Molecules* **2020**, *25*, 1009.

[7] Z. B. Wang, J. X. Liu, S. Grosjean, D. Wagner, W. Guo, Z. G. Gu, L. Heinke, H. Gliemann, S. Bräse, C. Wöll, *ChemNanoMat* **2015**, *1*, 338–345.

[8] a) H. H. Wenk, W. Sander, *Angew. Chem. Int. Ed.* **2002**, *41*, 2742–2745; b) E. Mendez-Vega, J. Mieres-Perez, S. V. Chapyshev, W. Sander, *Angew. Chem. Int. Ed.* **2019**, *58*, 12994–12998.

[9] a) H. Sato, R. Matsuda, K. Sugimoto, M. Takata, S. Kitagawa, *Nat. Mater.* **2010**, *9*, 661–666; b) T. Devic, O. David, M. Valls, J. Marrot, F. Couty, G. Férey, *J. Am. Chem. Soc.* **2007**, *129*, 12614–12615; c) T. Gadzikwa, O. K. Farha, C. D. Malliakas, M. G. Kanatzidis, J. T. Hupp, S. T. Nguyen, *J. Am. Chem. Soc.* **2009**, *131*, 13613–13615; d) H. C. Kolb, M. Finn, K. B. Sharpless, *Angew. Chem. Int. Ed.* **2001**, *40*, 2004–2021.

[10] a) C. Wentrup, *Angew. Chem. Int. Ed.* **2018**, *57*, 11508–11521; b) I. R. Dunkin, *Chem. Soc. Rev.* **1980**, *9*, 1–23.

[11] a) O. Shekhah, H. Wang, S. Kowarik, F. Schreiber, M. Paulus, M. Tolan, C. Sternemann, F. Evers, D. Zacher, R. A. Fischer, *J. Am. Chem. Soc.* **2007**, *129*, 15118–15119; b) O. Shekhah, H. Wang, M. Paradinas, C. Ocal, B. Schüpbach, A. Terfort, D. Zacher, R. A. Fischer, C. Wöll, *Nat. Mater.* **2009**, *8*, 481–484; c) O. Shekhah, H. Wang, D. Zacher, R. A. Fischer, C. Wöll, *Angew. Chem. Int. Ed.* **2009**, *48*, 5038–5041; d) R. A. Fischer, C. Wöll, *Angew. Chem. Int. Ed.* **2009**, *48*, 6205–6208.

[12] L. Heinke, Z. Gu, C. Wöll, *Nat. Commun.* **2014**, *5*, 4562.

[13] J. Liu, C. Wöll, *Chem. Soc. Rev.* **2017**, *46*, 5730–5770.

[14] a) M. Tsotsalas, J. Liu, B. Tettmann, S. Grosjean, A. Shahnas, Z. Wang, C. Azucena, M. Addicoat, T. Heine, J. Lahann, J. Overhage, S. Bräse, H. Gliemann, C. Wöll, *J. Am. Chem. Soc.* **2014**, *136*, 8–11; b) Deposition numbers 2264560 (before UV) and 2264561 (after UV) contain the supplementary crystallographic data for this paper. These data are provided free of charge by the joint Cambridge Crystallographic Data Centre and Fachinformationszentrum Karlsruhe Access Structures service.

[15] J. Liu, B. Lukose, O. Shekhah, H. K. Arslan, P. Weidler, H. Gliemann, S. Bräse, S. Grosjean, A. Godt, X. Feng, K. Mullen, I. B. Magdau, T. Heine, C. Wöll, *Sci. Rep.* **2012**, *2*, 921.
[16] a) Y. Wang, C. Wöll, *Chem. Soc. Rev.* **2017**, *46*, 1875–1932; b) Y. Wang, A. Glenz, M. Muhler, C. Wöll, *Rev. Sci. Instrum.* **2009**, *80*, 113108.
[17] a) P. O. Scokart, P. G. Rouxhet, *J. Chem. Soc. Faraday Trans.* **1980**, *76*, 1476–1489; b) D. Lin-Vien, N. B. Colthup, W. G. Fateley, J. G. Grasselli, *The handbook of infrared and Raman characteristic frequencies of organic molecules*, Elsevier, Amsterdam **1991**; c) R. Kostić, D. Raković, S. Stepanyan, I. Davidova, L. Gribov, *J. Chem. Phys.* **1995**, *102*, 3104–3109.
[18] R. Warmuth, S. Makowiec, *J. Am. Chem. Soc.* **2005**, *127*, 1084–1085.
[19] a) S. Bräse, K. Banert, *Organic Azides Syntheses And Applications*, Wiley, Hoboken **2010**; b) N. Gritsan, M. Platz, *Organic Azides Syntheses And Applications* (Eds.: S. Bräse, K. Banert), Wiley, hoboken **2010**, pp. 311–372.
[20] F. R. Benson, W. L. Savell, *Chem. Rev.* **1950**, *46*, 1–68.
[21] E. Leyva, M. S. Platz, G. Persy, J. Wirz, *J. Am. Chem. Soc.* **1986**, *108*, 3783–3790.
[22] a) E. D. Stenehjem, V. R. Ziatdinov, T. D. P. Stack, C. E. D. Chidsey, *J. Am. Chem. Soc.* **2013**, *135*, 1110–1116; b) J. P. Collman, N. K. Devaraj, T. P. Eberspacher, C. E. Chidsey, *Langmuir* **2006**, *22*, 2457–2464.
[23] I.-H. Park, E. Lee, S. S. Lee, J. J. Vittal, *Angew. Chem. Int. Ed.* **2019**, *58*, 14860–14864.
[24] a) N. J. Agard, J. A. Prescher, C. R. Bertozzi, *J. Am. Chem. Soc.* **2004**, *126*, 15046–15047; b) C. Liu, T. Li, N. L. Rosi, *J. Am. Chem. Soc.* **2012**, *134*, 18886–18888.
[25] a) H. Dong, M. Shen, J. E. Redford, B. J. Stokes, A. L. Pumphrey, T. G. Driver, *Org. Lett.* **2007**, *9*, 5191–5194; b) E. P. Farney, T. P. Yoon, *Angew. Chem. Int. Ed.* **2014**, *53*, 793–797.
[26] P. Kaszynski, D. A. Dougherty, *J. Org. Chem.* **1993**, *58*, 5209–5220.
[27] M.-L. Tsao, N. Gritsan, T. R. James, M. S. Platz, D. A. Hrovat, W. T. Borden, *J. Am. Chem. Soc.* **2003**, *125*, 9343–9358.
[28] a) L. Qiu, C. Yu, N. Zhao, W. Chen, Y. Guo, X. Wan, R. Yang, Y. Liu, *Chem. Commun.* **2012**, *48*, 12225–12227; b) Y.-Y. Lai, J.-M. Yeh, C.-E. Tsai, Y.-J. Cheng, *Eur. J. Org. Chem.* **2013**, 5076–5084.

Manuscript received: May 3, 2023
Accepted manuscript online: May 26, 2023
Version of record online: ■■, ■■

Research Articles

MOF Films

J. Song, X. Yu, A. Nefedov, P. G. Weidler, S. Grosjean, S. Bräse, Y. Wang,* C. Wöll* **e202306155**

Metal-Organic Framework Thin Films as Ideal Matrices for Azide Photolysis in Vacuum

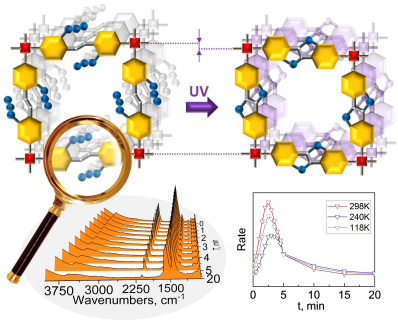

In the photo-mediated reactions of azides in well-designed Cu-(Da-SBDC) SURMOF matrices using a solvent-free approach the initial formation of the nitrene intermediate is shown to be followed by an intramolecular amination yielding an indoloindole. This work offers a novel strategy for precisely controlled chemical transformations of matrix-isolated azides in crystalline surface-mounted MOFs (SURMOFs).